Phase field simulations of stress controlling the vortex domain structures in ferroelectric nanosheets

W. J. Chen, Yue Zheng, and Biao Wang

Citation: Appl. Phys. Lett. **100**, 062901 (2012); doi: 10.1063/1.3681379
View online: http://dx.doi.org/10.1063/1.3681379
View Table of Contents: http://aip.scitation.org/toc/apl/100/6
Published by the American Institute of Physics

Articles you may be interested in

Switching mechanism of polarization vortex in single-crystal ferroelectric nanodots
Applied Physics Letters **97**, 192901 (2010); 10.1063/1.3515847

Phase field simulations of stress controlling the vortex domain structures in ferroelectric nanosheets

W. J. Chen, Yue Zheng,[a] and Biao Wang[b]
State Key Laboratory of Optoelectronic Materials and Technologies/Institute of Optoelectronic and Functional Composite Materials, and Micro&Nano Physics and Mechanics Research Laboratory, School of Physics and Engineering, Sun Yat-sen University, 510275 Guangzhou, China

(Received 21 October 2011; accepted 11 January 2012; published online 8 February 2012)

Effect of stress loads on the vortex domain structures (VDSs) in ferroelectric nanosheet has been investigated. Results of phase field simulations show that the different vortex domain structures can form in free-standing nanosheet from random perturbations. Applying stress loads on nanosheet, it is found that the domain morphology, especially the size and number of vortices, can be regularly controlled. These results indicate promising controlling the vortex domain structures in ferroelectric nanostructures by the mechanical loads. © *2012 American Institute of Physics*. [doi:10.1063/1.3681379]

Ferroelectric nanostructures (FNs) are attracting increasing attention for their original properties that can be exploited to develop functional devices.[1–5] Especially, low dimension FNs are found to exhibit vortex domain structures (VDSs).[6–11] With controlling the vortex patterns through external fields, such as its toroidal moment, it is promising to use these FNs to design novel nanoscale functional devices. Nevertheless, contrast with the magnetic dipole vortex phenomenon,[12,13] electric dipole vortex in low dimension FNs is just becoming a heating up topic, due to the challenge in experimental characterization and theoretical simulations.

The formation of VDS in low dimension FNs is due to the truncation of long-range interactions (electrostatic and elastic) at the surfaces, thus strongly depends on boundary conditions. In the literatures, the mechanism of forming VDS in FNs and effects of factors like boundary conditions and size have been theoretically studied by various methods. An effective Hamiltonian approach was employed to demonstrate the existence of VDS in nanoparticles, such as $BaTiO_3$ nanodots,[6] PZT nanodisks and nanorods.[7] The effect of boundary conditions on the forming of VDS in PZT nanodots and wires was also discussed.[14] Combining first-principles-based simulations and analytical derivations, Prosandeev and Bellaiche[15] determined the characteristics and signatures of VDS in ferroelectric nanodots. Based on the phenomenological theory, the VDS and vortex switching in FNs have also been simulated.[9,16]

Despite the well-known strong coupling between polarization and stress, regularity of the VDS in FNs controlled by the mechanical loads has not yet been investigated and discussed. Such kind of study should be instructive for future applications. In this letter, we present simulations on stress loads effect on the evolution and equilibrium of VDS in $BaTiO_3$ ferroelectric nanosheet (FNS) using a phase field model. Regularity of the stress loads on the domain morphology, size, and number of vortices in FNS have been discussed in depth.

In the following model, the spontaneous polarization $\mathbf{P} = (P_1, P_2, P_3)$ is chosen as the order parameter. Therefore, the electric displacement field $\mathbf{D}$ can be expressed as $\mathbf{D} = \varepsilon_b \mathbf{E} + \mathbf{P}$, where $\mathbf{E}$ is the electric field and ε_b the background dielectric constant tensor.[17,18] Since the background material is the cubic paraelectric phase, the background

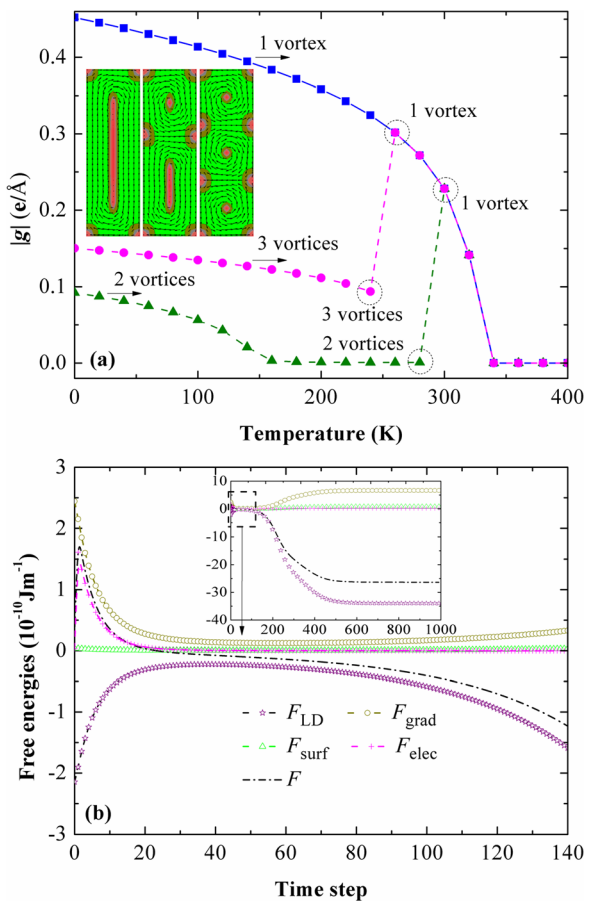

FIG. 1. (Color online) (a) Temperature dependence of toroidal moment of three VDSs in a free-standing FNS. The inserts depict the initial VDSs. (b) Evolution of free energies at the very beginning stage from random perturbation towards 1-vortex state. The insert depicts the evolution of free energies during a whole simulation.

[a]Electronic mail: zhengy35@mail.sysu.edu.cn.
[b]Electronic mail: wangbiao@mail.sysu.edu.cn.

 © 2012 American Institute of Physics

dielectric constants in three axis directions are the same, i.e., $\varepsilon_b = \varepsilon_{11b} = \varepsilon_{22b} = \varepsilon_{33b}$. Based on the phenomenological theory and taking into account effects of the mechanical stress, electric field, and surface, the total free energy of the FNS can be established as a sum of the Landau-Devonshire energy F_{LD}, gradient energy F_{grad}, electrostatic energy F_{elec}, and surface energy F_{surf}. An eighth-order polynomial of the modified Landau-Devonshire energy density as functions of the spontaneous polarizations and stresses can be expressed as[19–21]

$$\begin{aligned} f_{\mathrm{LD}} &= \alpha_1(P_1^2+P_2^2+P_3^2)+\alpha_{11}(P_1^4+P_2^4+P_3^4)+\alpha_{12}(P_1^2P_2^2+P_2^2P_3^2+P_1^2P_3^2) \\ &+ \alpha_{111}(P_1^6+P_2^6+P_3^6)+\alpha_{112}[P_1^2(P_2^4+P_3^4)+P_2^2(P_1^4+P_3^4)+P_3^2(P_1^4+P_2^4)] \\ &+ \alpha_{123}P_1^2P_2^2P_3^2+\alpha_{1111}(P_1^8+P_2^8+P_3^8)+\alpha_{1112}[P_1^6(P_2^2+P_3^2)+P_2^6(P_1^2+P_3^2) \\ &+ P_3^6(P_1^2+P_2^2)]+\alpha_{1122}(P_1^4P_2^4+P_2^4P_3^4+P_1^4P_3^4)+\alpha_{1123}(P_1^4P_2^2P_3^2+P_2^4P_1^2P_3^2 \\ &+ P_3^4P_1^2P_2^2)-Q_{11}(\sigma_{11}P_1^2+\sigma_{22}P_2^2+\sigma_{33}P_3^2)-Q_{12}[\sigma_{11}(P_2^2+P_3^2)+\sigma_{22}(P_1^2+P_3^2) \\ &+ \sigma_{33}(P_1^2+P_2^2)]-Q_{44}(\sigma_{23}P_2P_3+\sigma_{13}P_1P_3+\sigma_{12}P_1P_2)-s_{11}(\sigma_{11}^2+\sigma_{22}^2+\sigma_{33}^2)/2 \\ &- s_{12}(\sigma_{11}\sigma_{22}+\sigma_{22}\sigma_{33}+\sigma_{11}\sigma_{33})-s_{44}(\sigma_{12}^2+\sigma_{23}^2+\sigma_{13}^2)/2, \end{aligned} \tag{1}$$

where $\alpha_1 \equiv (T-T_{c0})/(2\varepsilon_0 C_0)$ is the dielectric stiffness, with T_{c0} and C_0 being the Curie-Weiss temperature and Curie-Weiss constant of the bulk material, and ε_0 the vacuum permittivity. α_{ij}, α_{ijk}, and α_{ijkl} are the higher-order stiffness coefficients. s_{ij} and Q_{ij} are the elastic compliance and electrostrictive coefficients, respectively. The stress field σ_{ij} is determined by the mechanical equilibrium equation, i.e., $\sigma_{ij,j}=0$, where the comma in the subscript denotes spatial differentiation.

The gradient energy represents the free energy contributed by the spatial polarization variation. To the lowest order of Taylor expansion, the gradient energy density takes the form as $f_{\mathrm{grad}} = g_{ijkl}P_{i,j}P_{k,l}/2$, with g_{ijkl} being the gradient energy coefficients. The electric energy density of a given polarization distribution is written as[17,22] $f_{\mathrm{elec}} = -\mathrm{P}_i\mathrm{E}_i - \frac{1}{2}\varepsilon_b\mathrm{E}_i\mathrm{E}_i$. Here, we neglect the free charge carriers, which might exist and have an influence on vortex formation and stability.[23] Under the open-circuit condition, the total electric field is equal to the depolarization field, which can be calculated for a free-charge-absent body by the electrostatic equilibrium equation as $D_{i,i}=0$. Due to truncation at the surface of the FNS, the spontaneous polarization is inhomogeneous across the out-of-plane direction. Thus, an additional surface energy is necessary to describe this intrinsic effect. Using the so-called extrapolation length δ_i^{eff}, the surface energy density of the FNS can be approximately given by $f_{surf} = \frac{D_{11}P_1^2}{2\delta_1^{eff}} + \frac{D_{22}P_2^2}{2\delta_2^{eff}} + \frac{D_{44}P_3^2}{2\delta_3^{eff}}$,[24] where D_{ij} are the material coefficients related to the gradient energy coefficients.

Integrating the free energy densities over the entire volume and surfaces yields the total free energy of the FNS as $F = \int_V (f_{\mathrm{LD}} + f_{\mathrm{grad}} + f_{\mathrm{elec}})dV + \int_S f_{\mathrm{surf}}dS$, with V and S being the volume and surface of the FNS, respectively. The temporal evolution of the spontaneous polarization field is described by the time-dependent Ginzburg-Landau (TDGL) equation,

$$\frac{\partial P_i}{\partial t} = -M\frac{\delta F}{\delta P_i}, (i=1,2,3) \tag{2}$$

where M is the kinetic coefficient and t is the time.

In the following simulations, we consider $BaTiO_3$ nanosheet under either traction free or stress loading boundary condition. Furthermore, open-circuit condition is employed to obtain a strong vortex effect. A two-dimensional 10×30 discrete grid points at a scale of $\Delta x = \Delta y = 1\mathrm{nm}$ is employed. The polarization evolution is solved numerically by discretizing the TDGL equation in time. At each time step, the stress and electrostatic fields are obtained by solving the mechanical and electrostatic equilibrium equations with given boundary conditions using finite element method. Values of the material coefficients in our simulation are listed in Ref. 25.[17,20,26]

For the FNS under traction-free condition at 0 K, result shows that different stable VDSs with one, two or three vortices (see the inserts in Fig. 1(a)) can form from various initial random perturbations. We are particular interested in how to switch these states into each other by changing the environment of the FNS. Using these three VDSs as initial

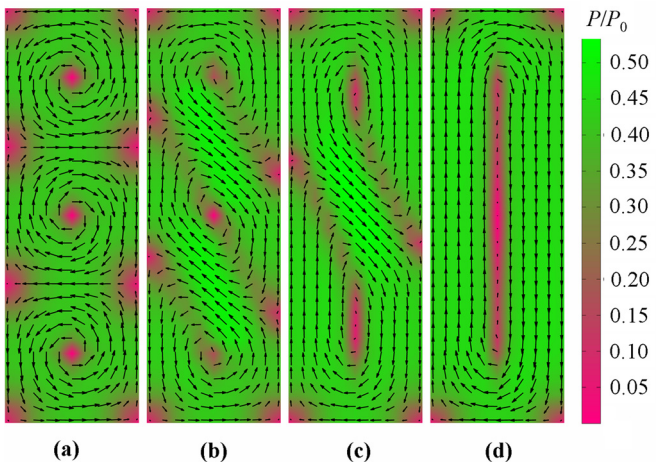

FIG. 2. (Color online) The equilibrium VDSs in a FNS with an initial 3-vortices state under tensile stress loads of (a) 0 GPa, (b) 0.5 GPa, (c) 1.0 GPa, and (d) 1.4 GPa.

states, we simulated their temperature stability, which can be characterized by the toroidal moment,[3] i.e., $\mathbf{g} = \frac{1}{V}\int_V \mathbf{r} \times \mathbf{P} dV$, with V being the volume of the system and $\mathbf{r}$ the position vector. The corresponding result is depicted in Fig. 1(a). Note that the 1-vortex state has a much larger toroidal moment than the other two states, since adjacent vortices tend to have anti-vortical directions to minimize the domain wall energy. At low temperature, the vortices in the 2-vortices state have different sizes, resulting a nonzero toroidal moment. The two vortices become to have same size as temperature increasing, thus a zero plateau of the toroidal moment appears. The 2-vortices and 3-vortices states are not stable at high temperature and sudden destabilize into the 1-vortex state at temperature around 280 K and 240 K, respectively. Moreover, the toroidal moment becomes zero at temperature around 340 K, manifesting the disappearing of the 1-vortex state. By tracing free energies during evolution from random perturbation toward the 1-vortex state as shown in Fig. 1(b), it can be seen that VDS forms to reduce the large electrostatic and gradient energies during the very beginning domain forming stage. Once the VDS forms, the electrostatic energy remains a small value compared with the other energies. It clearly indicates the important role of depolarization field in the vortex nucleation.

As seen from the above result, changing the ambient temperature can bring about vortex state transitions but in a single-directional way. It is interesting to investigate whether the transitions can be induced by mechanical loads. To accomplish this, we perform simulation of excreting a z-directional traction force τ on two surfaces of the FNS to let it in tensile or compressive strain state, which can be practically obtained by growing the FNS on a compliant substrate. Our result indicated that FNS having initial state with high vortex number is quite sensitive to the tensile stress loads. This is clearly depicted in Fig. 2 for FNS having an initial 3-vortices state (Fig. 2(a)). In particular, when τ is small (e.g., $\tau = 0.5$ GPa in Fig. 2(b)), the VDS remains 3-vortices but with a significant distortion, manifested by the strong tilt of the initial x-directional domains joining the vortices and an increase of polarization magnitude within. As τ increases to about 1.0 GPa (see Fig. 2(c)), the initial 3-vortices state destabilizes into a distorted "S-type" 2-vortices structure. We obtain a 1-vortex structure in the FNS when τ reaches 1.4 GPa, as shown in Fig. 2(d). Note that the VDSs in Fig. 2 are the equilibrium states with stress loads maintaining. Further result shows that, after removing the stress loads, the corresponding equilibrium states of the VDSs in Figs. 2(a)–2(d) are 3-vortices, 3-vortices, 2-vortices, and 1-vortex states. It can be seen that through applying tensile stress loads to the FNS, VDSs with more vortices can be successfully switched to VDSs with less vortices.

Contrast with the effect of tensile stress loads, compressive stress loads tends to increase the vortex number of the initial VDS. The simulation result for a FNS having an initial 1-vortex state is depicted in Fig. 3. It shows that with increasing the magnitude of the compressive traction τ, the initial 1-vortex state in the FNS can evolve into multi-vortices state. Specifically, the FNS is found to maintain 1-vortex structure when τ is between 0 GPa and −0.7 GPa (see Figs. 3(a) and 3(b)). However, it suddenly destabilizes into a 5-vortices structure when $\tau = 0.8$ GPa as shown in Fig. 3(c), and remains stable even τ reaches −4.0 GPa (Fig. 3(d)). We also found that the 5-vortices structure is not stable if the stress loads is removed and will evolve into 3-vortices state. This indicates that we can successfully switch the 1-vortex state into the 3-vortices state with compressive stress loads. Therefore, promising controlling the VDSs of FNS through compressive stress loads can be also achieved.

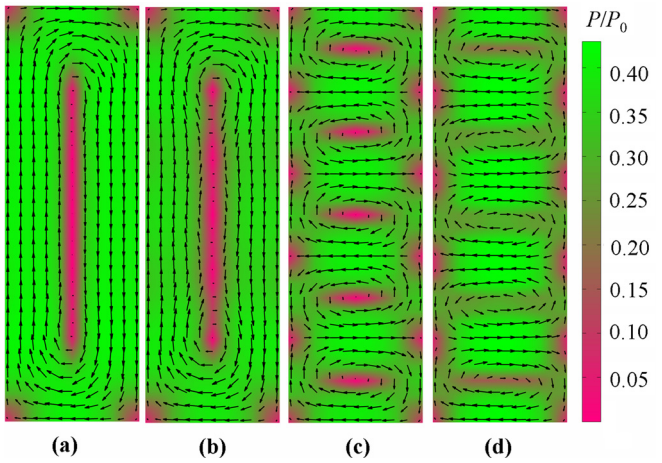

FIG. 3. (Color online) The equilibrium VDSs in a FNS with an initial 1-vortex state under compressive stress loads of (a) 0 GPa, (b) −0.7 GPa, (c) −0.8 GPa, and (d) −4.0 GPa.

In summary, effect of stress loads on the VDSs in FNS has been investigated using the phase-field simulations. For a given traction-free FNS, it is found that the equilibrium VDS depends on the initial random perturbations and temperature. The switching between these VDSs can be successfully achieved by stress loading and unloading. We believe that such effect revealed in nanosheet can be also found in other kinds of FNs with flatten configurations, and it also indicates promising stress controlling the VDS in FNs, such as nanobelt, nanowire, nanorod, and nanodot etc.

This project is grateful for support from NSFC (Nos. 10902128, 11072271, 10972239, and 51172291), FRF for the Central Universities, New Century Excellent Talents in University, and RF for the Doctoral Program of Higher Education.

[1]J. F. Scott, J. Phys.: Condens. Matter **18**, R361 (2006).
[2]E. Y. Tsymbal and H. Kohlstedt, Science **313**, 181 (2006).
[3]S. Prosandeev, I. Ponomareva, I. Naumov, I. Kornev, and L Bellaiche, J. Phys.: Condens. Matter **20**, 193201 (2008).
[4]P. M. Rørvik, T. Grande, and M. A. Einarsrud, Adv. Mater. **23**, 4007 (2011).
[5]Y. Zheng and C. H. Woo, Nanotechnology **20**, 075401 (2009); X. Luo, B. Wang, and Y. Zheng, ACS Nano **5**, 1649 (2011).
[6]H. Fu and L. Bellaiche, Phys. Rev. Lett. **91**, 257601 (2003).
[7]I. I. Naumov, L. Bellaiche, and H. Fu, Nature **432**, 737 (2004).
[8]S. Prosandeev, I. Ponomareva, I. Kornev, and L. Bellaiche, Phys. Rev. Lett. **100**, 047201 (2008).
[9]J. Wang and M. Kamlah, Phys. Rev. B **80**, 012101 (2009).
[10]A. Gruverman, D. Wu, H. J. Fan, I. Vrejoiu, M. Alexe, R. J. Harrison, and J. F. Scott, J. Phys.: Condens. Matter **20**, 342201 (2008).
[11]B. J. Rodriguez, X. S. Gao, L. F. Liu, W. Lee, I. I. Naumov, A. M. Bratkovsky, D. Hesse, and M. Alexe, Nano Lett. **9**, 1127 (2009).
[12]S. D. Bader, Rev. Mod. Phys. **78**, 1 (2006).
[13]C. L. Chien, F. Q. Zhu, and J. G. Zhu, Phys. Today **92**, 40 (2007).
[14]I. Ponomareva, I. I. Naumov, and L. Bellaiche, Phys. Rev. B **72**, 214118 (2005).

[15]S. Prosandeev and L. Bellaiche, Phys. Rev. B **75**, 094102 (2007).
[16]Y. Su and J. N. Du, Appl. Phys. Lett. **95**, 012903 (2009).
[17]Y. Zheng and C. H. Woo, Appl. Phys. A: Mater. Sci. Process. **97**, 617 (2009); C. H. Woo and Y. Zheng, Appl. Phys. A: Mater. Sci. Process. **91**, 59 (2008).
[18]A. K. Tagantsev, Ferroelectrics **375**, 19 (2008).
[19]M. J. Haun, E. Furman, S. J. Jang, H. A. McKinstry, and L. E. Cross, J. Appl. Phys. **62**, 3331 (1987).
[20]Y. L. Li and L. Q. Chen, Appl. Phys. Lett. **88**, 072905 (2006).
[21]Y. L. Wang, A. K. Tagantsev, D. Damjanovic, N. Setter, V. K. Yarmarkin, and A. I. Sokolov, Phys. Rev. B **73**, 132103 (2006).
[22]L. D. Landau, E. M. Lifshitz, and L. P. Pitaevskii, *Electrodynamics of Continuous Media* (Oxford University Press, Oxford, 1984).
[23]N. Balke, B. Winchester, W. Ren, Y. H. Chu, A. N. Morozovska, E. A. Eliseev, M. Huijben, R. K. Vasudevan, P. Maksymovych, J. Britson *et al.*, Nat. Phys. **8**, 81 (2012).
[24]R. Kretschmer and K. Binder, Phys. Rev. B **20**, 1065 (1979).
[25]$a_1 = 4.124(T - 388) \times 10^5$, $a_{11} = -2.097 \times 10^8$, $a_{12} = 7.974 \times 10^8$, $a_{111} = 1.294 \times 10^9$, $a_{112} = -1.950 \times 10^9$, $a_{123} = -2.5009 \times 10^9$, $a_{1111} = 3.863 \times 10^{10}$, $a_{1112} = 2.529 \times 10^{10}$, $a_{1122} = 1.637 \times 10^{10}$, $a_{1123} = 1.367 \times 10^{10}$, $s_{11} = 7.95 \times 10^{-12}$, $s_{12} = -4.305 \times 10^{-12}$, $s_{44} = 8.197 \times 10^{-12}$, $Q_{11} = 0.10$, $Q_{12} = -0.034$, $Q_{44} = 0.029$, $\delta_i^{eff} \approx 5 \times 10^{-9}$, $\varepsilon_b \approx 4.425 \times 10^{-10}$, $G_{11} = 3.46 \times 10^{-10}$, $G_{12} = 0$, and $G_{44} = G'_{44} = 1.73 \times 10^{-10}$ (in SI units).
[26]N. A. Pertsev, A. G. Zembilgotov, and A. K. Tagantsev, Phys. Rev. Lett. **80**, 1988 (1998).